A Matrix Converter Ride-Through Configuration Using Input Filter Capacitors as an Energy Exchange Mechanism

David Orser, *Member, IEEE*, and Ned Mohan, *Life Fellow, IEEE*

***Abstract*—A novel ride-through approach for matrix converters in adjustable speed drives is presented. The input capacitors are utilized to transfer energy from the spinning inertia of the motor to support the motor flux during grid fault events. The addition of three bidirection switches is required to isolate the input filter capacitors from the collapsed grid voltages. The addition of input switches, a ride-through vector control strategy, and post fault reconnection logic are shown to enable ride-through of many cycle faults without the use of an additional energy storage device. In this paper, the control and reconnect strategies are discussed followed by simulations of the system and the presentation of experimental results. Through a short review of power quality assessments, it is shown that these improvements allow matrix converter-based adjustable speed drives to operate in a majority of real world fault situations.**

***Index Terms*—AC machines, converters, drives, electric machines, energy storage, induction motors, inertial, matrix converters, motors, power conversion, ride-through, switching converters, variable-speed drives, zero voltage switching.**

I. Introduction

ADJUSTABLE speed drives (ASDs) are a growing segment of modern industrial infrastructure. The market for them is expected to be $18.8 billion by 2017 with a growth rate of approximately 8.7% [1]. ASDs are often more efficient, more reliable, and easier to control than other drives.

In today's environment, industrial ASDs are largely operated by voltage source inverter (VSI)-based power converters [2]. Matrix converters, introduced by Venturini in 1980, are capable of direct ac-to-ac conversion [3]. Unlike VSIs, matrix converters do not require an intermediate energy storage element. The lack of a bulky and relatively low reliability dc-link capacitor inherently gives matrix converters advantages which may be leveraged to improve size, cost, and reliability. Adoption continues to be slow, and presently only one company produces a commercial matrix converter [1]. The continuous advancement of power semiconductor technologies, including the recent commercialization of SiC MOSFETs [4], [5], will continue to make matrix converter-based architectures more attractive over time.

Many matrix converter problems have been identified and addressed in [6]. One major drawback of matrix converters is their lack of support for fault ride-through. Due to the lack of an energy storage element, any change in the input ac source directly impacts the output ac load. Without actively designing for fault ride-through support, fault events cause a rapid loss in torque and a reduction in flux in the motor. In the worst case, a complete loss of synchronism may occur. This will significantly impact the ability of the motor to recover beyond clearing of the grid fault, potentially requiring a complete stop and restart to occur [7].

Based on the source of energy utilized to sustain the system and the goal during ride-through events, fault ride-through can be split into two categories [8]:

1) *Residual Energy Ride-Through*: Energy is harvested from existing components of the system and the motor flux is maintained while minimizing cost.
2) *Stored Energy Ride-Through*: An external energy source is utilized, usually a large capacitor, battery backup, or secondary ac source. Often full torque output is made available to the system during ride-through.

As the main advantage of matrix converter-based ASDs is the lack of an energy storage element, this paper will address "residual energy ride-through."

Several solutions to the ride-through issue have previously been proposed. Holtz originally reviewed the issue of ride-through for back-to-back inverter-based power converters [9]. The dc link capacitor and the spinning inertia of the motor were utilized to sustain the system. Klumpner and Blaabjerg applied the same concept to matrix converters utilizing the clamp capacitor and zero vectors [7], [8]. Prasad *et al.* further developed this idea by applying a full suite of grid, zero, and open/clamp vectors in a hysteresis control method [10], [11]. However, in the later two cases, the clamp capacitor only reclaims power and cannot supply power to the motor due to the diode bridge connection. Cha and Enjeti added three additional switches and an additional dc capacitor to allow bidirectional power flow to the motor in ride-through operation [12], [13]. This modification required that a dc capacitor be added to the system. This capacitor or battery could be sized to meet any required ride-through capability. However, this resulted in effectively a stored energy ride-through solution.

This paper presents a new solution to grid fault ride-through for matrix converters in ASDs. It is shown that the input filter

Manuscript received April 25, 2014; revised July 10, 2014; accepted August 14, 2014. Date of publication August 29, 2014; date of current version March 5, 2015. This work was supported in part by the Office of Naval Research under Award N00014-11-1-0897, "Advanced Research in Power Electronic Systems for Naval Ships." Recommended for publication by Associate Editor U. K. Madawala.

The authors are with the Department of Electrical Engineering, University of Minnesota, Minneapolis, MN 55455 USA (e-mail: orse0009@umn.edu; mohan@umn.edu).

Color versions of one or more of the figures in this paper are available online at http://ieeexplore.ieee.org.

Digital Object Identifier 10.1109/TPEL.2014.2353054

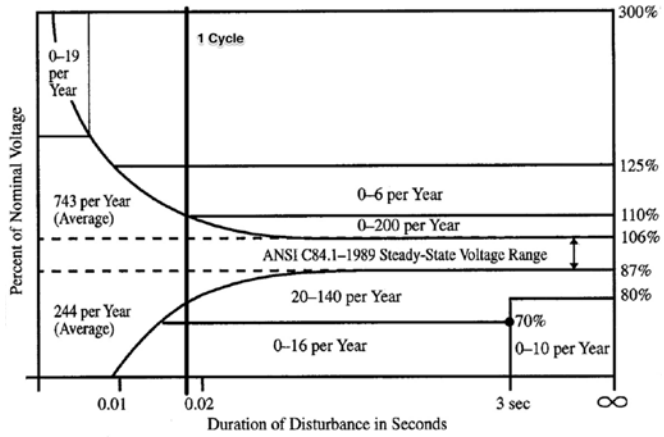

Fig. 1. Distribution of grid faults versus voltage and duration, image reproduced with permission from [16].

capacitors may be utilized as an energy transfer mechanism, with the addition of three bidirectional switches. A zero-power vector control strategy is utilized to harvest the required energy to support motor flux from the motor inertia in the presence of changing speed, voltage, and torque without requiring external energy from the filter capacitors. An on-the-fly grid reconnection strategy is employed to return to normal grid connections. In this paper, the solution is shown to ride-through grid faults of up to 0.5 s in duration with a 1-hp induction motor.

The general concept of this solution was presented previously [14]. This paper expands on the concept and shows the specific hardware implementation, including simulation results of the actual motor utilized in hardware. There are six sections. In Section II, a power survey is reviewed to identify the quantity, duration, and magnitude of grid faults. Section III discusses the three elements of the proposed solution, consisting of the input filter modifications, zero-power vector control, and on-the-fly reconnection strategy. Section IV describes the sequencing and vector control required during a fault event. Finally, Sections V and VI present the results of a full MATLAB Simulink system model and experimental results.

II. Surveying the Magnitude and Duration of Grid Faults

Grid faults come in many forms. Dorr *et al.* conducted a comprehensive study of fault type, duration, and magnitude in 1997 [15], [16]. This assessment draws on three power quality surveys by the National Power Laboratory, Canadian Electrical Association, and Electric Power Research Institute. Combined, these surveys consist of over 7000 monitor-months of data. Reviewing the data gives an overview of the importance of particular ride-through amplitude and duration targets. The summary of fault events can be seen in Fig. 1.

It should be noted that there are a number of fault regions that could be operable with only small changes to the design margins of the system and control electronics. Operating with electronics and switches that have slightly higher voltage ratings would cover faults in the 106 to 110% of nominal voltage region.

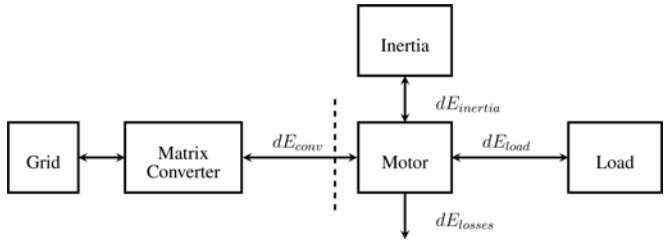

Fig. 2. Energy flow diagram.

Based on the data tables in [15], this accounts for 32% of all faults. Sizing motors such that they operate with 80% of the maximum ratings would allow operation in the 80 to 87% of nominal voltage region. This accounts for a further 56% of all faults.

Specifically, an ASD with the above changes and the presented ride-through methodology would cover a very large portion of all fault events (>95%, calculations based on Table III in [15]). To reach this level of coverage, this study will analyze low voltage faults of down to 0 p.u. for 0.5 s.

III. Proposed Ride-Through Solution

This section describes the following three components of the proposed solution:

1) Section III-A: input-filter-based voltage source to replace the grid during a fault event;
2) Section III-B: a zero-power vector control strategy to maintain flux in the motor and alignment information while no energy is available from the grid;
3) Section III-C: an on-the-fly reconnect strategy to resume normal operation after the fault has cleared.

The methods in Section III-A to isolate the matrix converter from the grid and the method in Section III-B to control the motor without using energy are highly interdependent. A short review of the control concept will help to understand the motivation behind the isolation method.

Looking at the change in energy at the motor described in Fig. 2, the energy balance equation can be written as

$$dE_{\text{inertia}} + dE_{\text{converter}} - dE_{\text{losses}} - dE_{\text{load}} = 0. \quad (1)$$

Given $dE = P\,dt$, setting dE to zero requires the power transfer to be zero at some point between the grid and motor, for example, the dashed line in Fig. 2. Assuming accurate control of the voltages and currents, the power transfer can be forced to zero. Doing so results in

$$dE_{\text{inertia}} = dE_{\text{losses}} + dE_{\text{load}}. \quad (2)$$

It can be seen that the losses and load will be inherently supplied with energy from the inertial energy of the system. Thus, this control scheme is referred to as zero-power control. The zero-power control scheme has the inherent advantage that it requires no external energy source to maintain the specified motor flux.

However, in reality, the stator currents of the induction machine cannot be controlled arbitrarily. A voltage source is required, essentially equal to the effective back EMF of the

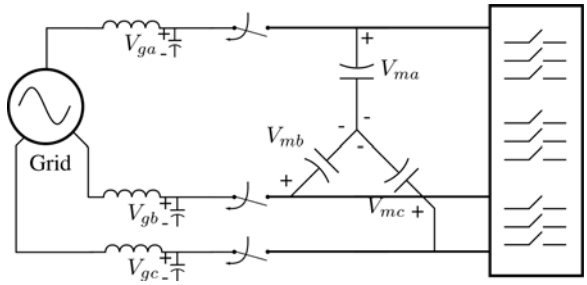

Fig. 3. Schematic of the three-phase input filter grid disconnect switches.

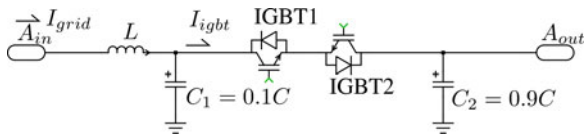

Fig. 4. Schematic of an IGBT implementation of a single phase of the grid disconnect switch.

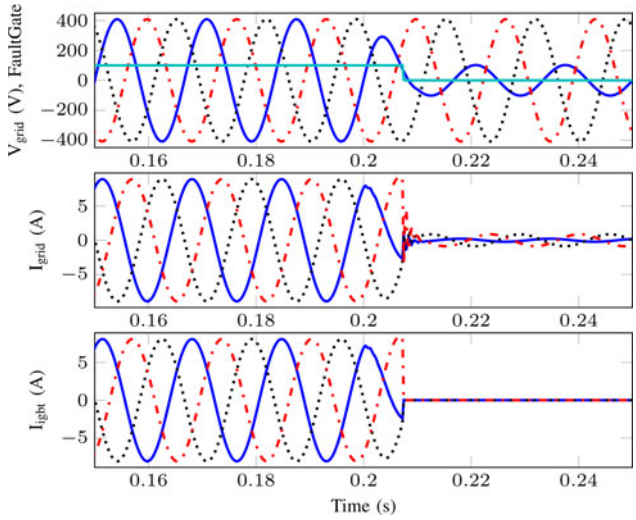

Fig. 5. Grid disconnect event: Input voltage and currents.

spinning motor in the presence of the specified flux. During a grid fault, one or more of the input phase voltages may be low or even zero, thus making control difficult or impossible [17]. An alternative voltage source is required. When utilizing zero-power control, this alternative voltage source is not required to provide any energy ($dE = 0$).

The alternative voltage source can be accomplished in number of ways. As discussed in Section I, this element has been implemented in other studies [7], [11], [13]. This paper will present the use of the input filter capacitor for this purpose.

A. Input-Filter-Based Voltage Source

The first element of the proposed solution is to provide an alternative source of voltage in the absence of the grid during a fault condition. A set of three switches between the grid and the filter capacitors is proposed as shown in Fig. 3.

These filter capacitors are required in matrix converters to make the input a voltage port. The input filter capacitors are typically large compared to clamp capacitors, but small compared to dc-link capacitors in conventional ASDs [18]. The proposed use of the input capacitors plus disconnect switches for ride-through will allow bidirectional power transfer to the motor during ride-through.

In the event a grid fault is detected, the switches are opened allowing the residual voltage present on the filter capacitors to be utilized by the converter. While these need to be bidirectional blocking switches, they only require switching speeds in excess of a fraction of the line frequency. This reduces the associated cost and losses. The switches can be implemented by nearly any semiconductor switching device, IGBTs, or MOSFETs. IGBTs were used in this paper.

At the moment of a disconnect event, a load current may be flowing in the inductor L. This current must be allowed to discharge slowly or it will cause an overvoltage condition. As shown in Fig. 4, it is recommended that there is a small capacitor to ground (see C_1 in Fig. 4) in order to discharge the remaining inductor current at the time of the disconnect event. During normal operation, the sum of C_1 and C_2 will be effectively equal to the designed filter capacitance value.

Simulations across power factor and fault phase angle were completed. No input over currents, over voltages, or other anomalies were found. An example simulation is shown in Fig. 5. In this simulation, a single phase fault on phase-a occurs and is detected. This is shown in Fig. 5 by the signal FaultGate transitioning low. At this time, the IGBTs open circuit and the current I_{igbt} immediately becomes zero. The current, I_{grid}, going through the inductor cannot immediately stop and is discharged into the C_1 capacitor, ringing slightly and decaying.

B. Zero-Power Control

As described previously, zero-power control consists of forcing the power transfer to be zero. This could be satisfied any place between the grid input terminals and the motor output terminals. However, in the basic vector control, the stator terminal voltages are directly controlled while measuring the stator terminal currents. Thus, voltage and current are known at this point, making it a convenient place to measure and control the power flow.

In standard rotor-aligned field-oriented control [19], [20], flux is controlled independently from torque, where i_{sd} controls flux and i_{sq} controls torque. The proposed zero-power control scheme operates only on torque, leaving flux to be controlled independently. A standard d-q or field oriented control scheme for ASDs is shown in Fig. 6. In zero-power control, the speed loop is replaced by a power loop as shown in Fig. 7. We will implement zero-power control by setting the input reference $P_{sdq,\mathrm{target}}$ to zero.

P_{sdq} is the power delivered by the matrix converter at the stator terminals defined as

$$P_{sdq} = v_{sd} i_{sd} + v_{sq} i_{sq}. \tag{3}$$

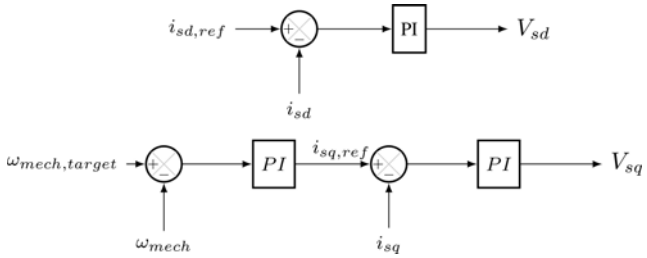

Fig. 6. Field-oriented control scheme (d-q), with speed control.

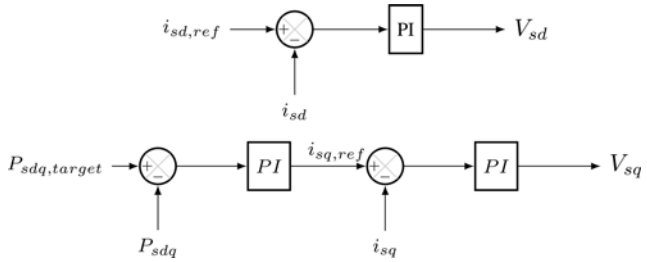

Fig. 7. Field-oriented control scheme (d-q), with zero-power control.

It can be shown that P_{sdq} is a squared function of i_{sq}. Therefore, linearization is needed in order to solve for $\frac{\Delta P_{sdq}}{\Delta i_{sq}}$.

In the Laplace domain, the standard form equations for d-q field-oriented control of an induction machine are

$$v_{sd} = R_s i_{sd} + s\lambda_{sd} - \omega_d \lambda_{sq} \tag{4}$$

$$v_{sq} = R_s i_{sq} + s\lambda_{sq} + \omega_d \lambda_{sd} \tag{5}$$

where λ_{sd} and λ_{sq} are defined in (6) and (7), assuming $\lambda_{rq} = 0$ (rotor d-axes-aligned flux model)

$$\lambda_{sd} = \sigma L_s i_{sd} + \frac{L_m}{L_r}\lambda_{rd} \tag{6}$$

$$\lambda_{sq} = \sigma L_s i_{sq} \tag{7}$$

and $\sigma = 1 - \frac{L_m^2}{L_r L_s}$.

With additional manipulation, not shown in the current manuscript [20], λ_{sd} can be written in terms of only i_{sd}

$$\lambda_{sd} = A(s) i_{sd} \tag{8}$$

where

$$A(s) = \frac{(\sigma L_s + L_m)(1 + \frac{\sigma L_s \tau_r}{\sigma L_s + L_m} s)}{(1 + s\tau_r))} \tag{9}$$

and

$$\tau_r = \frac{L_r}{R_r}. \tag{10}$$

Substituting λ_{sd} (8) and λ_{sq} (7) into v_{sd} (4) and v_{sq} (5) yields

$$v_{sd} = R_s i_{sd} + sA(s) i_{sd} - \omega_d \sigma L_s i_{sq} \tag{11}$$

$$v_{sq} = R_s i_{sq} + s\sigma L_s i_{sq} + \omega_d A(s) i_{sd}. \tag{12}$$

Substituting v_{sd} (11), v_{sq} (12), into the original equation for P_{sdq} (3), then taking the differential with respect to Δi_{sq} and

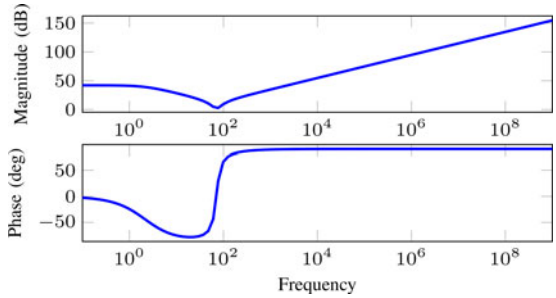

Fig. 8. Example zero-power control plant transfer function.

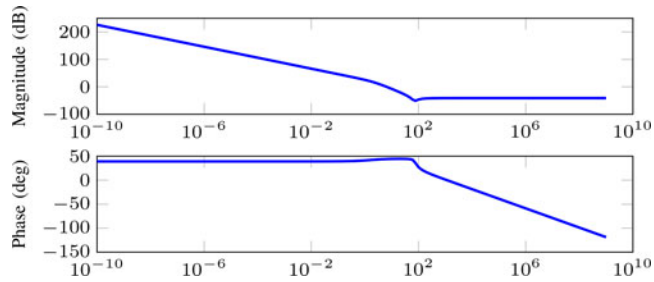

Fig. 9. Example zero-power control open-loop transfer function with controller.

ignoring Δ^2 terms yields

$$\frac{\Delta P_{sdq}}{\Delta i_{sq}} = -\omega_d \sigma L_s i_{sd} + (R_s + s\sigma L_s) 2 i_{sq} + \omega_d \frac{(\sigma L_s + L_m)(1 + \frac{\sigma L_s \tau_r}{\sigma L_s + L_m} s)}{(1 + s\tau_r))} i_{sd}. \tag{13}$$

This results in the plant response for the machine $\frac{\Delta P_{sdq}}{\Delta i_{sq}}$, shown in (13). Assuming selected machine parameters, the transfer function is shown in Fig. 8.

In the example shown, the plant contains predominately a left-half plane zero, thus is controllable by a single integrator (k_p/s). Adding this integrator and looking at the controller plus plant open-loop transfer function shown in Fig. 9, it can be seen that some gain remains at high-frequency, thus, an additional pole at high frequency could be added to improve gain margin.

Now that a transfer function has been obtained and a controller has been identified, the implementation of a ride-through scheme utilizing this control method can be realized.

The benefit of controlling for zero-power is twofold. First, the motor will support its own losses based entirely on its own inertia. Second, the voltage source, discussed in Section III-A, does not need to support any real power transfer. In addition, due to the orthogonal nature of field-oriented control, one can maintain a constant flux in the motor independent of the power control loop. The usefulness of this feature will be discussed further in the ride-through sequencing and control section of the paper below.

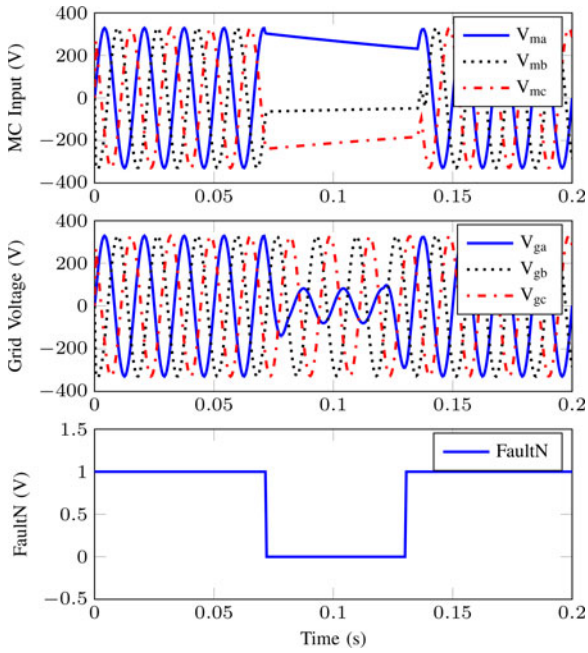

Fig. 10. Grid and capacitor voltages during fault event.

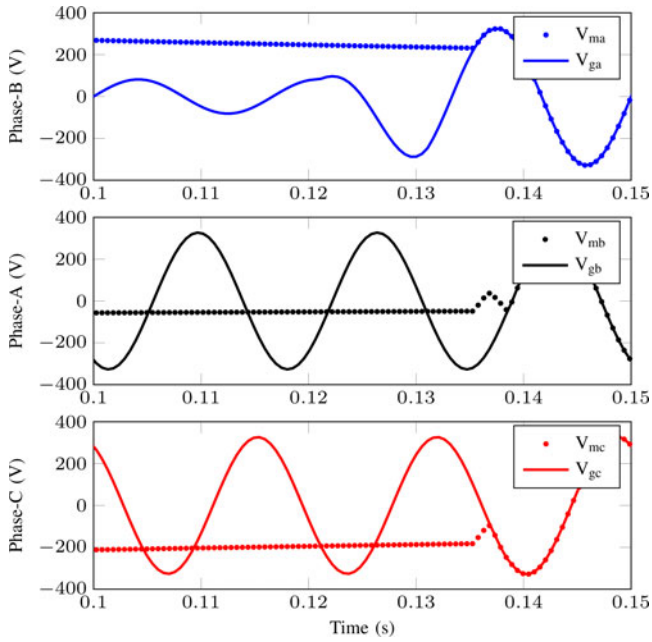

Fig. 11. Grid and matrix converter voltages during reconnections.

C. Reconnecting to the Grid

When the fault clears, the matrix converter must be reconnected to the grid. The voltages on the grid side of the disconnect switch are different than the voltages on the matrix converter side. Both sides of the switch have a moderate-sized capacitor on them (see Fig. 4). If the input switches should be reconnected arbitrarily, a large current will flow causing an overcurrent fault and potentially damaging the switch.

In order to facilitate a description of the reconnect strategy, t_d will be defined as the time at which the input switches are disconnected from the grid and t_c is the time at which the grid has returned to three-phase-balanced sinusoids and the fault has cleared. The node voltages for all three phases are denoted as V_{ga}, V_{gb}, V_{gc} (the grid side) and V_{ma}, V_{mb}, V_{mb} (matrix converter side) of the disconnect switch.

An example simulation is shown in Fig. 10, where $t_d = 0.07$ s and $t_c = 0.013$ s.

At t_d, the matrix converter inputs cannot be assumed to be balanced. In addition, as the fault progresses there will be small reductions in the isolated matrix converter voltages due to sensor network losses and other similar nonidealities. Due to these issues, $V_{m,abc}(t_c)$ cannot be assumed to be three-phase-balanced voltages. It is unlikely there will ever be a point in time when all three phases simultaneously match such that all three disconnect switches can be closed simultaneously. Furthermore, reconnecting at the wrong time could result in a total voltage collapse at the input terminals of the matrix converter. This would cause the motor currents to become uncontrolled, triggering faults and a loss of synchronism.

Thus, to determine the best time to reconnect the three disconnect switches, the following three conditions must be met:

1) overcurrents do not occur;
2) the virtual dc bus voltage should not decrease;
3) minimize reconnect time.

It is assumed that $V_{g,abc}(t > t_c)$ are sinusoidal and balanced with an A-B-C phase order. $V_{m,abc}(t_c)$ are assumed to be nearly dc with an amplitude less than $V_{m,abc}(t_d)$.

In order to facilitate the reconnect methodology, the case where $V_{ma} > V_{mb} > V_{mc}$ is analyzed. In this case, the matrix converter is operating on only the V_{ma} and V_{mc} phases. As stated from the second requirement above, the voltage between these two phases cannot be allowed to reduce during the reconnect event, otherwise the operation of the matrix converter may be impacted. For this to remain true, the highest-phase (A-phase) must reconnect while V_{ga} is increasing and the lowest phase (C-phase) must reconnect while V_{gc} is decreasing. The first requirement can be met by reconnecting each phase only when $V_{gx} \approx V_{mx}$. Restated, the phases will reconnect near zero voltage switching (ZVS) conditions.

Mathematically stated, the A-phase requirements are

$$\frac{\delta V_{ga}}{\delta t} > 0 \tag{14}$$

$$V_{ga} - V_{ma} \approx 0. \tag{15}$$

The C-phase requirements are

$$\frac{\delta V_{gc}}{\delta t} < 0 \tag{16}$$

$$V_{gc} - V_{mc} \approx 0. \tag{17}$$

The middle phase is less critical and only needs ZVS to occur

$$V_{gb} - V_{mb} \approx 0. \tag{18}$$

These requirements fundamentally define the best time to connect each phase individually. Due to the fact that these requirements occur each cycle, the reconnection must occur in a specific order to guarantee the second and third requirements.

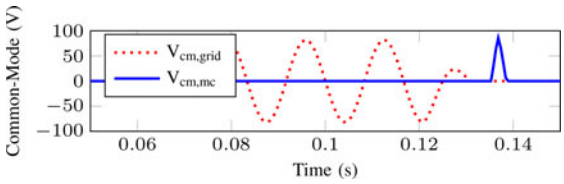

Fig. 12. Example of common-mode voltage during single phase fault event.

For the case $V_{ma} > V_{mb} > V_{mc}$, the correct connection order is ACB. If the switches were to reconnected in the CAB order, then there would be approximately 5/6 of a cycle where only one phase is connected. This would result in a prolonged common-mode voltage excursion and a total collapse of the virtual dc bus.

Shown in Fig. 11 is a detailed simulation zoomed in on the grid reconnect period.

During a proper reconnect, there is a short common-mode excursion as the first phase is connected, before the third phase is connected. However, this excursion is of the same order as the common-mode signal that results due to single phase fault. An example simulation is included in Fig. 12.

IV. Ride-Through Sequencing and Control

To successfully handle a ride-through event, there are a number of criteria that must be met [12]:

1) limit excessive currents;
2) minimize the disturbance to the load;
3) maintain the requested flux magnitude and alignment information;
4) at the end of fault, reaccelerate the motor.

Ride-through requires the system to accurately detect a fault in the grid. This could be done in a number of ways, but investigation into optimal fault detection in three-phase systems is outside the scope of this study. For the purposes of this paper, it is assumed that fault detection is in place. A fault is declared in the event any single phase drops below 0.9 p.u. of rated voltage amplitude.

When a fault is detected, the system will open the input switches and switch to zero-power control mode. The system maintains a constant flux by utilizing the system inertia. When the fault event clears, the input switches are closed and control is handed back to the speed controller. Both transitions require appropriate resetting of the integrators during mode transitions.

During fault operation, the matrix converter switching strategy is implemented as an indirect drive with active rectifier front-end. This allows for the absolute maximum available voltage to be made available for the motor driver output during fault events. No attempt to generate sinusoidal currents is possible in fault situations, due to the nonsinusoidal natures of the input voltages. During normal operation, any modulation strategy may be employed with this solution. The matrix control need only be switched between normal and fault modes at the time of the fault.

In the event that a very high output torque (i_{sq}) is present, it may be preferable to add an intermediate phase where torque is brought to zero in rate-limited manner, before handing control over to the zero-power controller. Alternatively, the reset value on the power-controller could be calculated in advance. In the simulations below, it was found unnecessary to include the zero torque stage. A direct handoff to the zero-power controller was implemented without problems.

TABLE I
Motor Parameters

		R_s	3.96 Ω
P	1 HP	R_r	2.45 Ω
V	230 V	L_{ls}	7.4 mH
p	4 poles	L_{lr}	11.1 mH
		L_m	162 mH

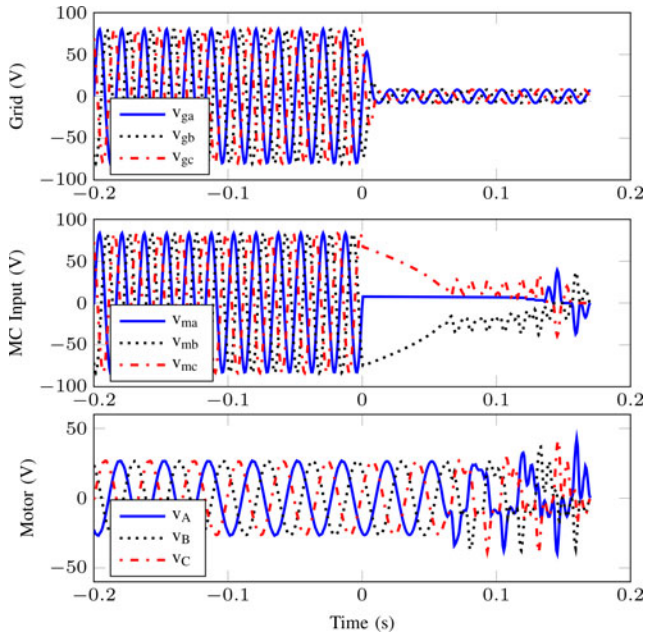

Fig. 13. No ride-through control: Zoomed in terminal voltages of a 0.5-s three-phase fault.

V. Full System Modeling Results

Simulations of a three-phase induction motor, matrix converter, and input disconnect switches were completed. The machine parameters utilized are listed in Table I.

An average-model matrix converter [21], [22] was utilized. This model was a reasonable choice for 5-20 second mode switching and control simulations, where switching characteristics are not needed and lead to much longer simulation times. MATLAB Simulink was used to simulate the motor model and control systems. The integrated version of the PLECs simulator was used to simulate the power electronics. The motor was operated during a three phase 0.1 p.u. fault of 0.5 s at an initial speed of 90 rad/s. The inertia utilized in the simulation was approximately that of the induction motor, the dc motor, and the coupling used for characterization.

The simulations shown in Figs. 13 and 14 contrast the addition of zero-power control. The simulation shown in Fig. 13 shows

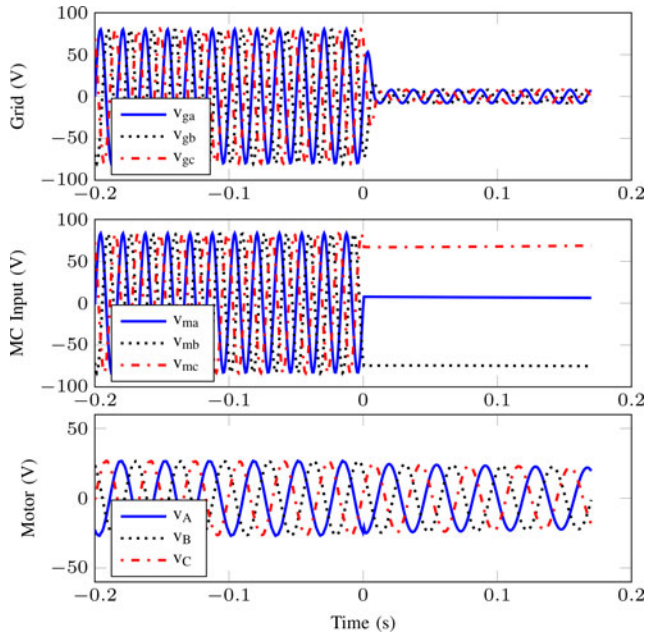

Fig. 14. Proposed ride-through control: Zoomed in terminal voltages of a 0.5-s three-phase fault.

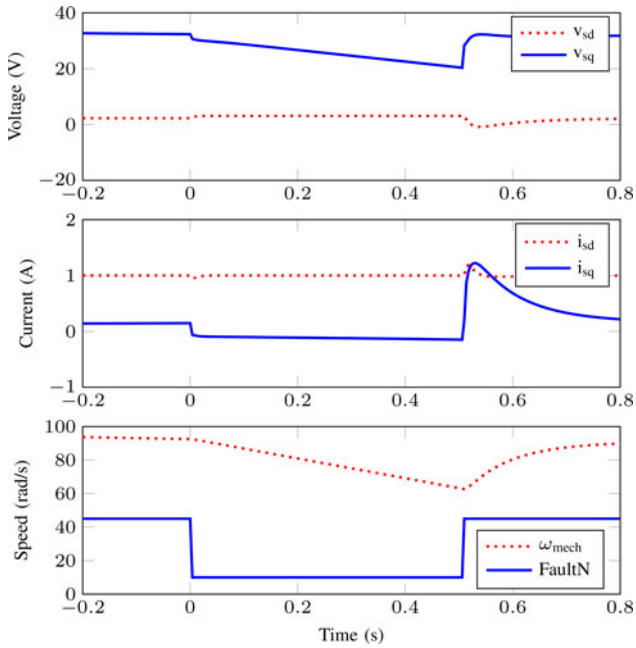

Fig. 15. Proposed ride-through control: Vector control parameters of a 0.5-s three-phase fault.

a normal matrix converter-driven, speed-controlled motor in the presence of the grid fault. As can be seen, the matrix converter input voltage collapses within 0.05 s. Control of the motor is lost due to the inability of the matrix converter to provide the commanded voltages to the motor.

Returning to the proposed solution, Fig. 14 shows the response to the same 0.5-s fault, but with the full proposed ride-through solution. The vector control quantities are shown in Fig. 15. Torque goes from positive to slightly negative keeping the capacitor voltage from collapsing. The proposed solution resulted in a loss of speed of 30 $\mathrm{rad/s}$ over the duration of the fault. It can be seen that during a grid fault with a long duration, the system is limited by the total inertia available to the system.

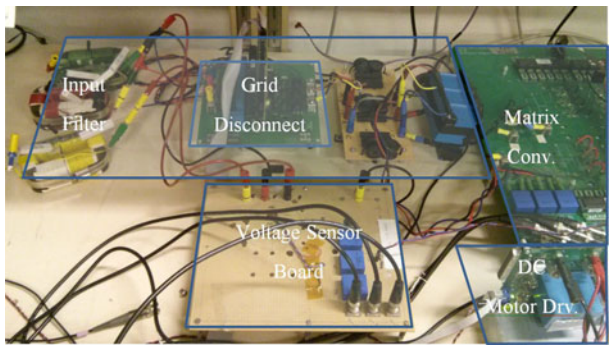

Fig. 16. Photo of experimental hardware: Input filter, disconnect board, and matrix converter.

VI. Experimental Results

The hardware consists of several independent components, listed below:

1) input disconnect switches and filter;
2) matrix converter with indirect drive modulation scheme;
3) 1-hp DC motor coupled to 1-hp ac induction machine;
4) DC motor driver and controller;
5) fault sequence controller;
6) control loop hardware.

The disconnect board is implemented with IGBT switches and contains the input side 10% capacitors. The filter components are discrete, as are the grid side voltage sensors, shown in Fig. 16. The matrix converter board is realized by IGBTs switches and contains the matrix converter input voltage sensors and output current sensors. The matrix converter modulation scheme is Implemented on FPGA1 utilizing XILINX ISE. The disconnect logic, safety logic, and DC motor driver controller are implemented on FPGA2 utilizing XILINX System Generator. Finally, the control loops are implemented by a DSPACE DS1104 rapid prototyping system utilizing MATLAB Simulink.

The motors, shown in Fig. 17, are a Baldor VECTOR Drive induction motor and a Leeson permanent magnet DC motor.

A 0.5-s grid fault is created by the input grid disconnect switch, during which the DSPACE controller is given a signal to switch into ride-through mode. The control mode switches to zero-power control and waits until the fault is declared over. The reconnect logic then takes over and sequentially reconnects the phases of the matrix converter. When the reconnect is complete, the DSPACE controller is switched back into normal operation.

In the three-phase waveform, shown in Fig. 18, there is a transient response due to the system's initial positive i_{sq} that must rapidly slew to slightly below zero, resulting in overshoot. The available voltage on the capacitor has an integrated component

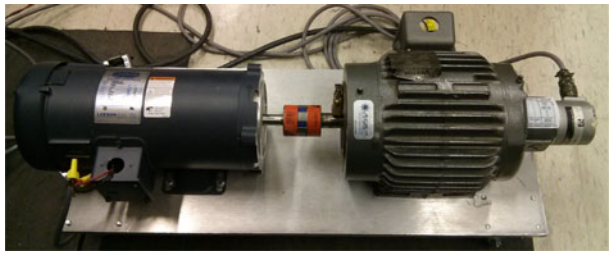

Fig. 17. Photo of experimental hardware: 1-hp motors.

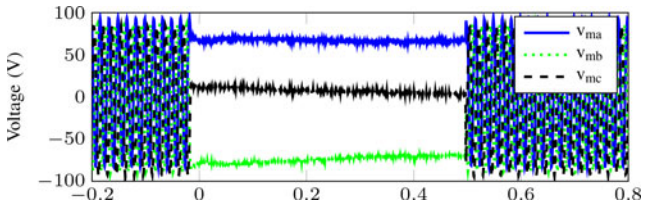

Fig. 18. Experimental results: Matrix converter input voltages during a 0.5-s fault and recovery.

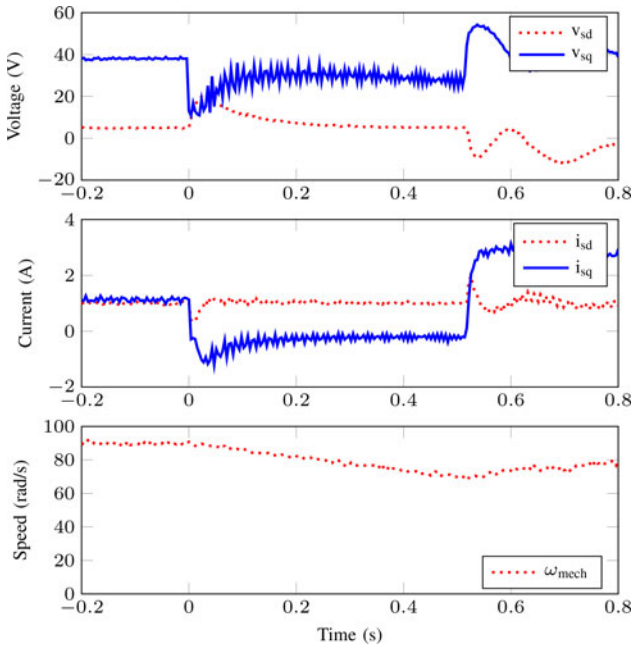

Fig. 19. Experimental results: Vector control parameters during a 0.5-s fault and recovery.

due to this dynamic response of the power loop, thus, a voltage limiter may be needed. A voltage limiter may also be useful in the case that the speed controller is regenerating energy from the load at the time of disconnect (negative i_{sq}). This extra energy could be limited and utilized to recharge the filter capacitors and extend ride-through duration.

The hardware shows no faults and operates correctly for faults up to 0.5 s in duration. An example is shown in Fig. 19. This is primarily limited by the inertia available within the tested motors.

VII. Component Considerations

Selection of the input disconnect switches is not difficult but there are some considerations that need to be briefly addressed. The steady-state energy requirement of the capacitors is zero due to zero-power control. However, in transitioning from high output torque to slightly negative output torque, there is a transient need for energy from the filter capacitors. The size of the input capacitors is predominately dependent on the transient overshoot of the system. If following the design recommendations in [18], [23], which choose the capacitor values based on limiting of the RMS harmonic current injected into the grid, the capacitors should be of sufficient size to handle these transients.

Internal losses in the electronics and sensor resistor bridges can impact the residual voltage on the capacitors as well. In the event internal losses are substantial enough to impact the residual voltage on the capacitors, the power target $P_{sdq,\mathrm{target}}$ (typically zero) can be adjusted to a slightly negative value to compensate and maintain available voltage. This results in a small reduction of ride-through duration.

The switches need to be rated for a maximum voltage of the line-to-line voltage plus applicable margins. Current rating for the switches should be rated values as well. Since the switching of the input disconnect circuits only needs to occur within a small portion of the input line frequency (1 ms or approximately 1000 Hz), the grid disconnect switches can be set up for a significantly slower switching time than the main matrix converter switches (typically 10 kHz or faster). This will allow the disconnect switches to be sized for approximately ten times lower conduction losses than the main matrix converter switches, yielding approximately 1.1 times the conduction losses of a standard matrix converter without ride-through support. The grid disconnect switches will add no additional switching losses in normal operation.

VIII. Conclusion

This paper has introduced the use of the matrix converter, input filter capacitors as an energy exchange mechanism to enable ride-through of grid faults in ASDs. The use of these capacitors requires the addition of three bidirectional switches between the filter capacitors and inductors. A novel zero-power control scheme maintains the specified flux while harvesting the requisite energy from the inertia of the drive. This control scheme automatically harvests the correct amount of energy to support losses even in the presence of changing voltage, current, and mechanical speed. An on-the-fly reconnection strategy is employed to allow for safe and immediate reconnection of the grid after the fault is cleared.

Individual components simulations, a MATLAB Simulink Model of the overall system, and experimental results are presented. They show a matrix converter fed ASD successfully rides through a 0.5-s three-phase grid fault. Through reviewing three power quality studies, the above improvements provide adequate coverage of the majority of fault situations.

REFERENCES

[1] Yaskawa. (2008). Application note: AC7 matrix converter. [Online]. Available: http://www.yaskawa.com/attachments/AN.AC7.01.pdf

[2] A. von Jouanne, P. Enjeti, and B. Banerjee, "Assessment of ride-through alternatives for adjustable-speed drives," *IEEE Trans. Ind. Appl.*, vol. 35, no. 4, pp. 908–916, Jul./Aug. 1999.

[3] M. Venturini, "A new sine wave in, sine wave out, conversion technique eliminates reactive elements," in *Proc. 7th Nat. Solid-State Power Convers. Conf.*, 1980, pp. E3-1–E3-15.

[4] S. Safari, A. Castellazzi, and P. Wheeler, "Experimental and analytical performance evaluation of SiC power devices in the matrix converter," *IEEE Trans. Power Electron.*, vol. 29, no. 5, pp. 2584–2596, May 2014.

[5] T. E. Salem and R. A. Wood, "1000-H evaluation of a 1200-V, 880-A all-SiC dual module," *IEEE Trans. Power Electron.*, vol. 29, no. 5, pp. 2192–2198, May 2014.

[6] P. Wheeler, J. Rodriguez, J. Clare, L. Empringham, and A. Weinstein, "Matrix converters: A technology review," *IEEE Trans. Ind. Electron.*, vol. 49, no. 2, pp. 276–288, Apr. 2002.

[7] C. Klumpner and F. Blaabjerg, "Experimental evaluation of ride-through capabilities for a matrix converter under short power interruptions," *IEEE Trans. Ind. Electron.*, vol. 49, no. 2, pp. 315–324, Apr. 2002.

[8] C. Klumpner, I. Boldea, and F. Blaabjerg, "Short term ride through capabilities for direct frequency converters," in *Proc. Power Electron. Spec. Conf.*, 2000, pp. 235–241.

[9] J. Holtz, W. Lotzkat, and S. Stadtfeld, "Controlled AC drives with ride-through capability at power interruption," *IEEE Trans. Ind. Appl.*, vol. 30, no. 5, pp. 1275–1283, Oct. 1994.

[10] R. Prasad, K. Basu, K. K. Mohapatra, and N. Mohan, "Ride-through study for matrix-converter adjustable-speed drives during voltage sags," in *Proc. 36th Annu. Conf. IEEE Ind. Electron. Soc.*, Nov. 2010, pp. 686–691.

[11] R. Prasad, "Low voltage ride-through capability for matrix converter fed adjustable-speed induction machine drives for industrial and wind applications," Ph.D. dissertation, Dept. Elect. Eng., Univ. Minnesota, Minneapolis, MN, USA, 2011.

[12] H. J. Cha and P. Enjeti, "A new ride-through approach for matrix converter fed adjustable speed drives," in *Proc. Ind. Appl. Conf.*, Oct. 2002, pp. 2555–2560.

[13] H. Cha and P. Enjeti, "Matrix converter-fed ASDs," *IEEE Ind. Appl. Mag.*, vol. 10, no. 4, pp. 33–39, Jul. 2004.

[14] D. Orser and N. Mohan, "Utilizing inertial energy to extend ride-through for matrix converters in adjustable speed drives," in *Proc. 7th IEEE GCC Conf. Exhib.*, Nov. 2013, pp. 611–616.

[15] D. Dorr, "Power quality study-1990 to 1995-initial results," in *Proc. 7th Annu. Appl. Power Electron. Conf. Expo.*, 1992, pp. 303–308.

[16] D. Dorr, M. Hughes, T. Gruzs, R. Jurewicz, and J. McClaine, "Interpreting recent power quality surveys to define the electrical environment," *IEEE Trans. Ind. Appl.*, vol. 33, no. 6, pp. 1480–1487, Dec. 1997.

[17] N. Kumar, T. Chelliah, and S. Srivastava, "Voltage sag effects on energy-optimal controlled induction motor with time-varying loads," in *Proc. IEEE Int. Conf. Power Electron., Drives Energy Syst.*, Dec. 2012, pp. 1–6.

[18] A. Sahoo, K. Basu, and N. Mohan, "Comparison of filter components of back-to-back and matrix converter by analytical estimation of ripple quantities," in *Proc. 39th Annu. Conf. IEEE Ind. Electron. Soc.*, Nov. 2013, pp. 4831–4837.

[19] O. Wasynczuk, S. Sudhoff, T. Tran, D. Clayton, and H. Hegner, "A voltage control strategy for current-regulated PWM inverters," *IEEE Trans. Power Electron.*, vol. 11, no. 1, pp. 7–15, Jan. 1996.

[20] N. Mohan. Hoboken, NJ, USA: Wiley, Aug. 2014.

[21] S. Thuta, "*Simplified control of matrix converter and investigations into its applications*," Ph.D. dissertation, Dept. Elect. Eng., , Univ. Minnesota, Minneapolis, MN, USA, 2007.

[22] N. Mohan, *Power Electronics: A First Course*. Hoboken, NJ, USA: Wiley, 2012.

[23] K. Basu, A. K. Sahoo, V. Chandrasekaran, and N. Mohan, "Grid-side ac line filter design of a current source rectifier with analytical estimation of input current ripple," *IEEE Trans. Power Electron.*, vol. 29, no. 12, pp. 6394–6405, Dec. 2014.

David Orser (S'99–M'01) received the B.S. degree in electrical engineering from the Minnesota State University, Mankato, MN, USA, in 2000, the M.S. degree in electrical engineering from the University of Minnesota , Twin Cities, MN, USA, in 2007, and is currently working toward the Ph.D. degree in electrical engineering at the University of Minnesota.

He currently works at MISO Energy, Eagan, MN, as a Senior Engineer. He has worked for more than ten years in high-speed analog IC design for IBM and LSI. He has researched and taught at the University of Minnesota and Minnesota State University in both microelectronics and power electronics. He holds five patents and has two IEEE publications. His research interests include matrix converters in electric drives and the application of power electronics in HVDC power systems.

Ned Mohan (S'72–M'73–SM'91–F'96–LF'12) received the B.Tech. degree from the Indian Institute of Technology, Kharagpur, India, in 1967, the M.S. degree in electrical engineering from the University of New Brunswick, Fredericton, NB, Canada, in 1969, and the M.S. degree in nuclear engineering and the Ph.D. degree in electrical engineering from the University of Wisconsin, Madison, WI, USA, in 1972 and 1973, respectively.

He is currently the Oscar A. Schott Professor of power electronics at the University of Minnesota, Minneapolis, MN, USA, where he has been engaged in teaching since 1976.

He received the 2008 IEEE-PES Outstanding Educator Award, 2010 IEEE Undergraduate Teaching Award, and 2012 IEEE Power and Energy Society Ramakumar Family Renewable Energy Excellence Award. In 2013, he received the Innovative Program Award from the ECE Department Heads Association. In 2014, he received the IEEE PES Nari Hingorani FACTS Award. He is a Member of the National Academy of Engineering.